www.ietdl.org

Published in IET Science, Measurement and Technology
Received on 31st May 2011
Revised on 27th January 2012
doi: 10.1049/iet-smt.2011.0114

Special Issue on Computation in Electromagnetics containing selected, extended papers from CEM 2011

ISSN 1751-8822

Comparative analysis of $A - V$ and $A - T - T_0$ calculations of induced currents in multiply connected regions

R.M. Wojciechowski[1] *A. Demenko*[1] *J.K. Sykulski*[2]

[1]*Poznan University of Technology, ul. Piotrowo 3A, 60-965 Poznan, Poland*
[2]*University of Southampton, Southampton SO17 1BJ, UK*
E-mail: jks@soton.ac.uk; j.k.sykulski@soton.ac.uk

Abstract: The study offers a comparative analysis of two methods, both using potentials, for electromagnetic field computation in multiply connected regions, including a conventional $A - V$ approach and a fairly new and much less popular $A - T - T_0$ formulation. The relevant finite element equations are provided which are solved using the BR-ICCG method combining block relaxation with the ICCG algorithm. To facilitate comparisons the TEAM Workshop Problem No. 7 has been solved and the results of both formulations verified by measurements. The computational times have been considered.

1 Introduction

The formulations relying on potential are most commonly used in the analysis of electromagnetic fields. There are three basic possibilities: (a) the $\Omega - T$ description, where the magnetic field is described by the scalar potential Ω, whereas the electric field in terms of the electric vector potential T; (b) the probably best known $A - V$ formulation, with the vector potential A describing the magnetic field and the electric scalar potential V applied to the electric field; and (c) the $A - T$ description utilising both vector potentials. The $A - V$ approach has dominated the analysis of induced currents in three dimensions mainly because of the simplicity and universality of the associated finite element (FE) algorithm. Moreover, the procedures for solving simply and multiply connected regions are similar. The disadvantage of the $A - V$ formulation arise from inefficient computation, a result of slow convergence of the iterative scheme of solving the FE equations [1]. On the other hand, the $A - T$ and $\Omega - T$ methods are ill suited to the calculations of induced currents in multiply connected regions [1, 2]. The classical T description needs to be supplemented by auxiliary equations in terms of the electric vector potential T_0 describing the current distribution around the 'holes' of the multiply connected volumes [2, 3]. As a result a joint $T - T_0$ formulation has emerged [2], slowly gaining popularity. A popular alternative, when analysing systems with holes in terms of the vector potential T, is to fill the holes with a material of very low, but finite, conductivity [4]. After the hole has been replaced by a 'fictitious' very weakly conducting material the whole region becomes strongly non-homogenous, but quasi-coherent and thus the eddy currents may be computed conveniently using the classical T formulation. However, this method has been shown to be less accurate and computationally more time consuming than the proposed $T - T_0$ approach [5].

The authors of this article have been searching for more efficient formulations of the $A - T - T_0$ description by utilising the edge values of the vector potentials; these have been shown to be competitive with other well-established methods. Here we focus on the comparison of performance of our own algorithms based on the $A - T - T_0$ formulation with $A - V$ computations employing the edge values of the vector potential A and the nodal values of the scalar potential V. The comparative analysis has been conducted using the example of TEAM Workshop Problem No. 7 [6] (Fig. 1), for which the differential equations in terms of complex variables with linear coefficients have been derived. The equations have been solved using the BR-ICCG algorithm for formulation applying complex potentials. The computing times and accuracy have been compared for both the considered formulations.

The FE equations have been set up following [7, 8] and described using the language of circuit theory. The FE equations arising from the scalar formulation and nodal elements are equivalent to the nodal equations of an edge network (EN) constructed from the branches associated with element edges (Fig. 2*a*); whereas the equations for the vector potentials for the system described by the edge elements are represented by the loop equations of the facet network (FN) made of the branches joining the element mid-points (Fig. 2*b*).

2 FE equations for the $A - V$ formulation

The FE equations based on the use of the magnetic vector potential A and electric scalar potential V are equivalent to the loop equations of the magnetic FN coupled with the nodal equations of the EN [7]. The coupling between the

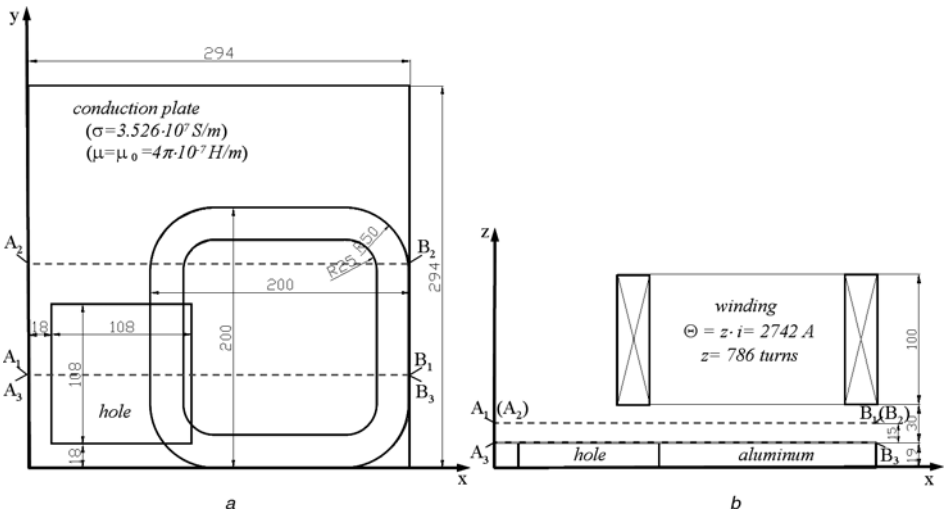

Fig. 1 *TEAM Workshop Problem No. 7 – asymmetrical conductor with a hole [6]*

a Plane view
b Front view

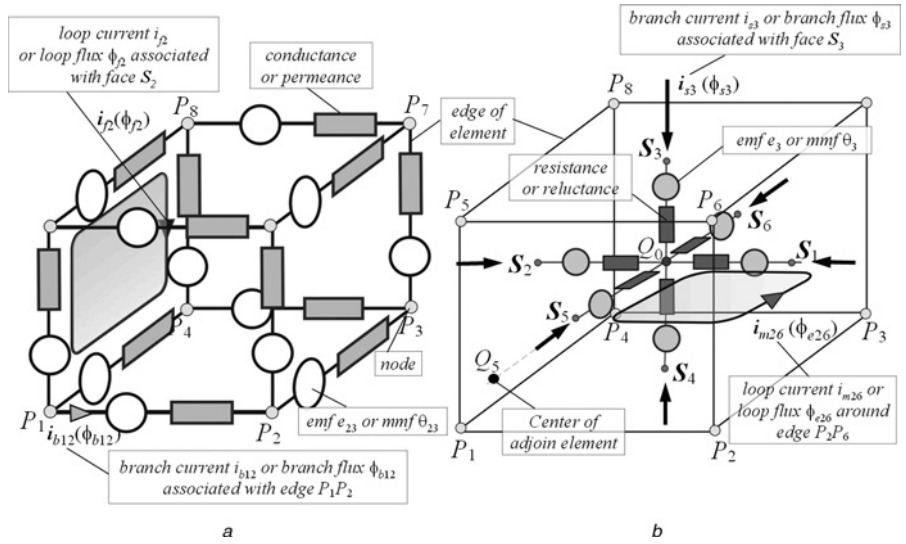

Fig. 2 *Circuit models of hexahedron*

a Edge
b Facet

networks is provided by the sources and the equations may be written as

$$\begin{bmatrix} \boldsymbol{k}_{\mathrm{n}}^{\mathrm{T}}\boldsymbol{G}_{\mathrm{g}}\boldsymbol{k}_{\mathrm{n}} & -\dfrac{\partial}{\partial t}\boldsymbol{k}_{\mathrm{n}}^{\mathrm{T}}\boldsymbol{G}_{\mathrm{g}} \\ -\boldsymbol{G}_{\mathrm{g}}\boldsymbol{k}_{\mathrm{n}} & \boldsymbol{k}_{\mathrm{e}}^{\mathrm{T}}\boldsymbol{R}_{\mu}\boldsymbol{k}_{\mathrm{e}} + \dfrac{\partial}{\partial t}\boldsymbol{G}_{\mathrm{g}} \end{bmatrix} \begin{bmatrix} \boldsymbol{V} \\ \boldsymbol{\phi}_{\mathrm{e}} \end{bmatrix} = \begin{bmatrix} \boldsymbol{0} \\ \boldsymbol{\theta}_{\mathrm{m}} \end{bmatrix} \quad (1)$$

where $\boldsymbol{V}$ is the vector of nodal potentials, $\boldsymbol{\phi}_{\mathrm{e}}$ represents the loop fluxes, that is edge values of $\boldsymbol{A}$, $\boldsymbol{G}_{\mathrm{g}}$ is the matrix of branch conductances in EN, $\boldsymbol{R}_{\mu}$ is the matrix of branch reluctances of the FN, $\boldsymbol{k}_{\mathrm{n}}$ is the transposed nodal incidence matrix of EN and $\boldsymbol{k}_{\mathrm{e}}$ is the transposed loop matrix for FN. The symbol $\boldsymbol{\theta}_{\mathrm{m}}$ represents the vector of the external loop mmfs. In this approach the branch conductances are found using the interpolating functions of the edge elements, whereas the branch reluctances on the basis of the interpolating functions of the facet elements. Having solved (1), the currents $\boldsymbol{i}_b$ in the branches of the EN network, that is the currents related to the edges of the elements (see Fig. 3), may be established from the nodal values of potential $\boldsymbol{V}$ and the edge values of the loop fluxes $\boldsymbol{\phi}_{\mathrm{e}}$, while the following relationship holds

$$\boldsymbol{i}_b = \boldsymbol{G}_{\mathrm{g}}\left(\boldsymbol{k}_{\mathrm{n}}\boldsymbol{V} - \frac{\partial}{\partial t}\boldsymbol{\phi}_{\mathrm{e}}\right) \quad (2)$$

3 FE equations for the $A - T - T_0$ formulation

The FE equations for the edge elements and the vector potentials $\boldsymbol{A}$, $\boldsymbol{T}$ and $\boldsymbol{T}_0$ are equivalent to the loop equations of the coupled magnetic and electric FNs. In the electric network, a distinction has to be made between the equations for the loops around the element edges and those surrounding the 'hole' in the multiply connected case. The loop currents $\boldsymbol{i}_{\mathrm{m}}$ around the element edges represent the edge values of the potential $\boldsymbol{T}$, whereas the currents $\boldsymbol{i}_{\mathrm{o}}$ embracing the 'hole' correspond to the edge values of the potential $\boldsymbol{T}_0$. The derivation of the currents $\boldsymbol{i}_{\mathrm{o}}$ may follow either of two equivalent formulations, where the description

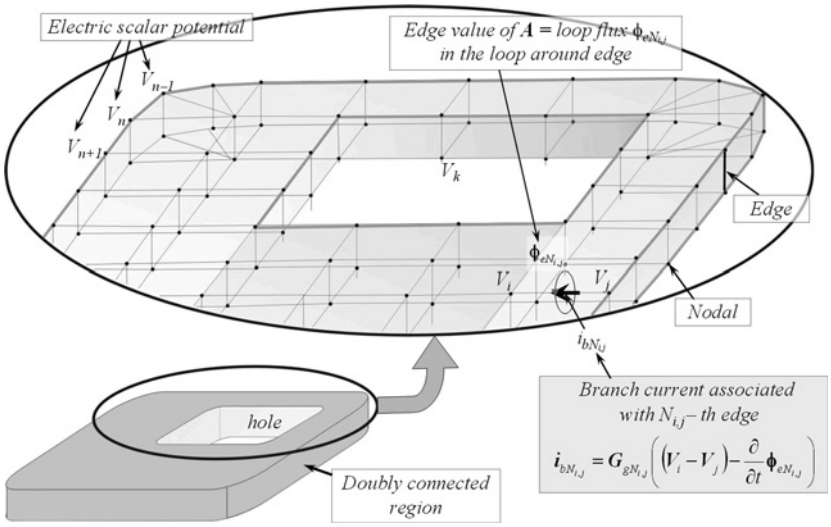

Fig. 3 *Representation of a multiply connected region in the edge electric network (EN)*

of the loops may be linked to: (a) cuts of the loop surfaces around the holes with element edges, or (b) cuts of the loop edges around the holes with element facets. These derivations are explained in detail in [2, 5]. Here we follow the latter description (Fig. 4) and the FE equations have been written as

$$\begin{bmatrix} \boldsymbol{k}_{\mathrm{e}}^{\mathrm{T}}\boldsymbol{R}_{\rho}\boldsymbol{k}_{\mathrm{e}} & \boldsymbol{k}_{\mathrm{e}}^{\mathrm{T}}\boldsymbol{R}_{\rho}\boldsymbol{z}_{\mathrm{f}} & \frac{\partial}{\partial t}\boldsymbol{k}_{\mathrm{e}}^{\mathrm{T}}\boldsymbol{K} \\ \boldsymbol{z}_{\mathrm{f}}^{\mathrm{T}}\boldsymbol{R}_{\rho}\boldsymbol{k}_{\mathrm{e}} & \boldsymbol{z}_{\mathrm{f}}^{\mathrm{T}}\boldsymbol{R}_{\rho}\boldsymbol{z}_{\mathrm{f}} & \frac{\partial}{\partial t}\boldsymbol{z}_{\mathrm{f}}^{\mathrm{T}}\boldsymbol{K} \\ -\boldsymbol{K}^{\mathrm{T}}\boldsymbol{k}_{\mathrm{e}} & -\boldsymbol{K}^{\mathrm{T}}\boldsymbol{z}_{\mathrm{f}} & \boldsymbol{k}_{\mathrm{e}}^{\mathrm{T}}\boldsymbol{R}_{\mu}\boldsymbol{k}_{\mathrm{e}} \end{bmatrix} \begin{bmatrix} \boldsymbol{i}_{\mathrm{m}} \\ \boldsymbol{i}_{\mathrm{o}} \\ \boldsymbol{\phi}_{\mathrm{e}} \end{bmatrix} = \begin{bmatrix} \boldsymbol{0} \\ \boldsymbol{0} \\ \boldsymbol{\theta}_{\mathrm{m}} \end{bmatrix} \tag{3}$$

where $\boldsymbol{R}_{\mu}$ and $\boldsymbol{R}_{\rho}$ are the matrices of the branch reluctances and resistances of relevant FNs obtained using the interpolating functions of the FE, $\boldsymbol{z}_{\mathrm{f}}$ is the matrix describing the distribution of the loops around the 'holes' defined on the basis of the cuts of the loops around the holes with element facets and $\boldsymbol{K}$ is a matrix transposing the branch values – that is the facet values of flux and/or current densities – of the FN into the values related to the branches of the EN [9], that is currents and/or fluxes associated with the element edges. In the proposed formulation the currents $\boldsymbol{i}_{\mathrm{s}}$ in the electric FN, that is the branch currents passing through the facets of the elements (Fig. 4), may be found from the loop currents $\boldsymbol{i}_{\mathrm{m}}$ and $\boldsymbol{i}_{\mathrm{o}}$ using

$$\boldsymbol{i}_{\mathrm{s}} = \boldsymbol{k}_{\mathrm{e}}\boldsymbol{i}_{\mathrm{m}} + \boldsymbol{z}_{\mathrm{f}}\boldsymbol{i}_{\mathrm{o}} \tag{4}$$

It should be noted that the difference between the formulations $\boldsymbol{A} - V$ and $\boldsymbol{A} - \boldsymbol{T} - \boldsymbol{T}_0$ applies only to the equations describing the flow of the induced currents. To find the current distributions a nodal method is used in $\boldsymbol{A} - V$, whereas a loop scheme in $\boldsymbol{A} - \boldsymbol{T} - \boldsymbol{T}_0$. Moreover, in setting up the loop equations the ungauged formulation is applied. In the language of circuit theory we could say that an overspecified loop matrix is used as a consequence of the singular formulation [10]. General algorithms based on the vector potential $\boldsymbol{A}$ often utilise the procedures for solving the redundant equations for the vector potential $\boldsymbol{A}$ [11]. The introduction of additional loops in the method based on the vector potential results in significant acceleration of the convergence of the algorithm. This idea has been extended here and applied to the $\boldsymbol{A} - \boldsymbol{T} - \boldsymbol{T}_0$ formulation. Original procedures have been developed for solving such singular formulations for both the equations

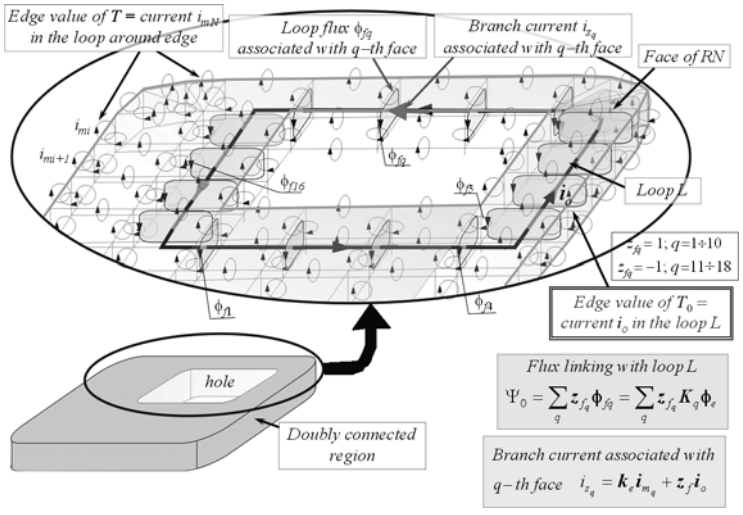

Fig. 4 *Representation of a multiply connected region in a facet electric network (FN)*

doi: 10.1049/iet-smt.2011.0114

describing the vector potential $\boldsymbol{A}$ and the potentials $\boldsymbol{T}$ and $\boldsymbol{T}_0$. The benefits are described later in this article.

4 BR-ICCG method

The authors have developed a special version of the BR − ICCG method in order to solve the equations for the edge values of potentials using the $\boldsymbol{A} - \boldsymbol{T} - \boldsymbol{T}_0$ formulation and implemented it in their own codes. The method is universal and may be applied to the analysis of harmonic-induced currents using complex potentials, as well as to the systems requiring time discretisation. The procedure will be explained and illustrated using the complex notation where $\partial/\partial t \Rightarrow \mathrm{j}\omega$. In the BR-ICCG method the system of (3) is divided into two blocks: (a) one that includes the equations in terms of the magnetic vector potential $\boldsymbol{A}$

$$\boldsymbol{R}_{\mu\mathrm{o}}\underline{\boldsymbol{\phi}}_{\mathrm{e}} = \underline{\boldsymbol{\theta}}_{\mathrm{m}} + N^{\mathrm{T}}\underline{\boldsymbol{i}}_{\mathrm{m}} + \boldsymbol{E}_{\mathrm{o}}^{\mathrm{T}}\underline{\boldsymbol{i}}_{\mathrm{o}} \tag{5}$$

and (b) a second block that includes the equations arising from the potentials $\boldsymbol{T} - \boldsymbol{T}_0$

$$\begin{bmatrix} \boldsymbol{R}_{\rho\mathrm{o}} & \boldsymbol{R}_{\mathrm{w}}^{\mathrm{T}} \\ \boldsymbol{R}_{\mathrm{w}} & \boldsymbol{R}_{\mathrm{oc}} \end{bmatrix} \begin{bmatrix} \underline{\boldsymbol{i}}_{\mathrm{m}} \\ \underline{\boldsymbol{i}}_{\mathrm{o}} \end{bmatrix} = \begin{bmatrix} -\mathrm{j}\omega N\underline{\boldsymbol{\phi}}_{\mathrm{e}} \\ -\mathrm{j}\omega \boldsymbol{E}_{\mathrm{o}}\underline{\boldsymbol{\phi}}_{\mathrm{e}} \end{bmatrix} \tag{6}$$

When subdividing (3) into the above two blocks it was assumed that $\boldsymbol{R}_{\mu\mathrm{o}} = \boldsymbol{k}_{\mathrm{e}}^{\mathrm{T}}\boldsymbol{R}_{\mu}\boldsymbol{k}_{\mathrm{e}}$, $N = \boldsymbol{k}_{\mathrm{e}}^{\mathrm{T}}\boldsymbol{K}$, $\boldsymbol{E}_{\mathrm{o}} = \boldsymbol{z}_{\mathrm{f}}^{\mathrm{T}}\boldsymbol{K}$, $\boldsymbol{R}_{\rho\mathrm{o}} = \boldsymbol{k}_{\mathrm{e}}^{\mathrm{T}}\boldsymbol{R}_{\rho}\boldsymbol{k}_{\mathrm{e}}$, $\boldsymbol{R}_{\mathrm{w}} = \boldsymbol{z}_{\mathrm{f}}^{\mathrm{T}}\boldsymbol{R}_{\rho}\boldsymbol{k}_{\mathrm{e}}$.

In the proposed approach each block is further divided into smaller sub-blocks related to specified groups of the edges [12]. With the aim to achieve simplicity of the final equations for the sub-blocks it is beneficial to use hexahedral elements so that the element edges coincide with the axes of the coordinate system (Fig. 5), as sub-blocks are then formed from the equations related to the layers perpendicular to a given group of the edges. The equations for the layers may be written as for a two-dimensional model with additional sources representing the couplings between layers. In the case of the electric vector potential $\boldsymbol{T}$ the extra sources also include terms resulting from the interaction between loop equations around the edges of the given layer and equations for the loops around the singular regions, that is, the equations for the potential $\boldsymbol{T}_0$. The number of loops around these singular regions is normally much smaller than the number of loops for the $\boldsymbol{T}$ formulation. Moreover, the current path in a single additional loop (a loop representing the edge value of the potential $\boldsymbol{T}_0$) may be passing through more layers, not necessarily associated with one group of the edges. It was decided therefore that it would not make much sense to subdivide the equations further into sub-blocks because of the loops around the holes and thus all the equations relating to the $\boldsymbol{T}_0$ method belong to one sub-block of the second block of (3). Finally, although the method has been illustrated here using the hexahedral elements, the approach may also be applied to the prism elements, or when a mixture of the hexahedral and prism elements is used. The only difference relates to the choice of layers for setting up the equations for sub-blocks.

The division of the block into sub-blocks is illustrated below using an example of the second block [refer to (6)] with the equations describing the edge values of the electric vector potentials, which – after the subdivision into layers – take the form

$$\begin{bmatrix} \boldsymbol{R}_{\rho\mathrm{o}_{xx}} & \boldsymbol{R}_{\rho\mathrm{o}_{xy}} & \boldsymbol{R}_{\rho\mathrm{o}_{xz}} & \boldsymbol{R}_{\mathrm{w}_x}^{\mathrm{T}} \\ \boldsymbol{R}_{\rho\mathrm{o}_{yx}} & \boldsymbol{R}_{\rho\mathrm{o}_{yy}} & \boldsymbol{R}_{\rho\mathrm{o}_{yz}} & \boldsymbol{R}_{\mathrm{w}_y}^{\mathrm{T}} \\ \boldsymbol{R}_{\rho\mathrm{o}_{zx}} & \boldsymbol{R}_{\rho\mathrm{o}_{zy}} & \boldsymbol{R}_{\rho\mathrm{o}_{zz}} & \boldsymbol{R}_{\mathrm{w}_z}^{\mathrm{T}} \\ \boldsymbol{R}_{\mathrm{w}_x} & \boldsymbol{R}_{\mathrm{w}_y} & \boldsymbol{R}_{\mathrm{w}_z} & \boldsymbol{R}_{\mathrm{oc}} \end{bmatrix} \cdot \begin{bmatrix} \underline{\boldsymbol{i}}_{\mathrm{m}_x} \\ \underline{\boldsymbol{i}}_{\mathrm{m}_y} \\ \underline{\boldsymbol{i}}_{\mathrm{m}_z} \\ \underline{\boldsymbol{i}}_{\mathrm{o}} \end{bmatrix} = -\mathrm{j}\omega \begin{bmatrix} \boldsymbol{0} & \boldsymbol{N}_{xy} & \boldsymbol{N}_{xz} \\ \boldsymbol{N}_{yx} & \boldsymbol{0} & \boldsymbol{N}_{yz} \\ \boldsymbol{N}_{zx} & \boldsymbol{N}_{zy} & \boldsymbol{0} \\ \boldsymbol{E}_{\mathrm{o}_x} & \boldsymbol{E}_{\mathrm{o}_y} & \boldsymbol{E}_{\mathrm{o}_z} \end{bmatrix} \cdot \begin{bmatrix} \underline{\boldsymbol{\phi}}_{\mathrm{e}_x} \\ \underline{\boldsymbol{\phi}}_{\mathrm{e}_y} \\ \underline{\boldsymbol{\phi}}_{\mathrm{e}_z} \end{bmatrix} \tag{7}$$

where $\boldsymbol{R}_{\rho\mathrm{o}_{uu}}$ ($u, v = x, y, z$) is a matrix of coefficients of the uth group of the sub-blocks consisting of the sub-matrices ($\boldsymbol{R}_{\rho\mathrm{o}_{uu}}$) ($q$th layer) for the sub-blocks, the matrix $\boldsymbol{R}_{\rho\mathrm{o}_{uv}}$

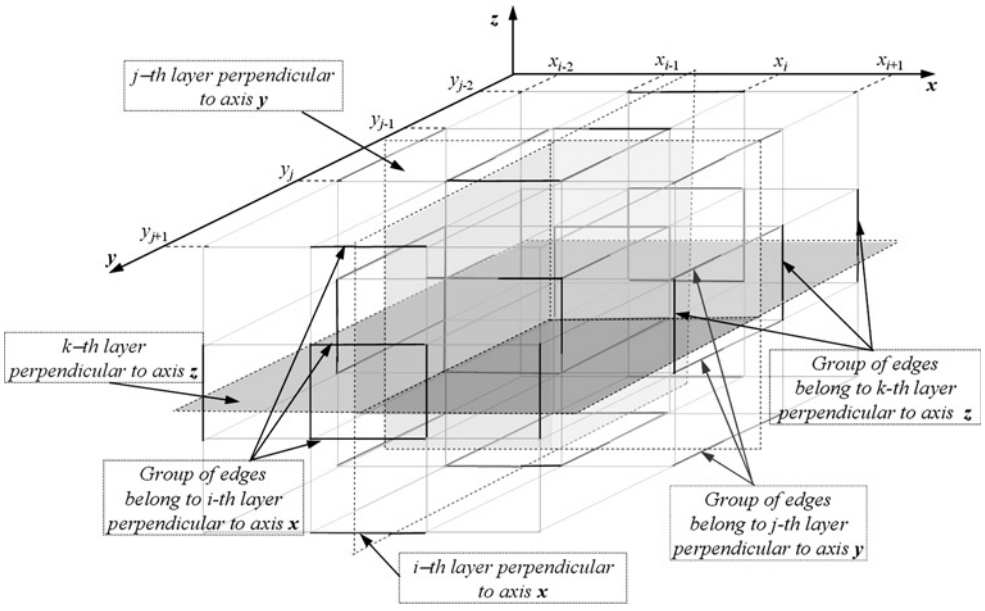

Fig. 5 *Portion of the mesh showing the three layers perpendicular to the coordinates*

describes the mutual terms between the sub-blocks belonging to different groups, and $\boldsymbol{R}_{w_u}$ is a matrix of the mutual terms between the layers of the uth group and the equations of the loops around the singular regions. The matrix $\boldsymbol{N}_{uv}$ is a sub-matrix of the matrix $\boldsymbol{N}$ and consists of the sub-matrices $(\boldsymbol{N}_{uv})_q$ related to the sub-blocks. The sub-matrix $(\boldsymbol{N}_{uv})_q$ transforms the loop currents (fluxes) of the FN into the currents (fluxes) associated with those branches of the EN which are related to the edge of the qth sub-block of the uth group of the sub-blocks. In the case of the subdivision into layers as in Fig. 5 the main diagonal elements of the matrix $\boldsymbol{N}$ are all zero as the sub-vector $\boldsymbol{\phi}_{eu}$ of the loop fluxes related to the uth group of the sub-blocks (uth component) is not present in the expression describing the right-hand side of the uth system of equations of the current flow field. The matrix $\boldsymbol{E}_{o_u}$ is a sub-matrix of $\boldsymbol{E}_o$ and refers to the uth group of the sub-blocks, that is to a group of the edges and the edge values of which are used to define the flux coupled with the ith additional loop.

The BR-ICCG algorithm itself is fairly straightforward; in a given iteration step the equations are solved sequentially for the sub-blocks (layers), first for the block describing the edge values of the vector potential $\boldsymbol{A}$ and then for the second block containing the edge values of $\boldsymbol{T}$ and $\boldsymbol{T}_0$, whereas the equations for the sub-blocks are solved using the complex ICCG method. It is worth observing that using the proposed way of forming the sub-block equations makes the complex ICCG method equivalent to the IC-preconditioned conjugate orthogonal conjugate gradient method [13]. When solving the equations for the qth layer the right-hand side vector is formed from the previously computed solutions. The iterations terminate when the norm of the error ε drops below a specified value ε_z; in the cases reported here the termination value was assumed to be $\varepsilon_z = 10^{-5}$. One of the benefits of the above algorithm is the relative ease with which parallel computation may be incorporated – for example by simultaneous solution of sub-block equations – which leads to saving in computing times. The details of the implementation of parallel processing are not discussed here.

The algorithm for the $\boldsymbol{A} - V$ method, with which the new $\boldsymbol{A} - \boldsymbol{T} - \boldsymbol{T}_0$ formulation has been compared, is very similar, with the only difference relating to the way in which the second block (describing the equations of the V formulation) is solved. The equations for the current flow field are also solved using complex ICCG, although no subdivision into smaller blocks was applied because of a known slow convergence of a block relaxation method when applied to the classical FE formulation.

5 Results and comparison of methods

The TEAM Workshop Problem No. 7 [6] (Fig. 1) has been solved using both formulations ($\boldsymbol{A} - V$ and $\boldsymbol{A} - \boldsymbol{T} - \boldsymbol{T}_0$) and the results are compared with the measurements published in [14]. Parallelepiped elements have been used resulting in about half a million equations for the edge values of the vector potential $\boldsymbol{A}$, 20 000 for the scalar potential V and 63 000 for the edge values of $\boldsymbol{T} - \boldsymbol{T}_0$. Complex potentials were used throughout and the equations were solved using the elaborated BR-ICCG method. Figs. 6–8 present the computed and measured selected distributions: (a) of the magnetic flux density B_z along the line $A_1 - B_1$, (b) of the magnetic flux density B_z along the line $A_2 - B_2$ and (c) of the current density J_y along the line $A_3 - B_3$, for two frequencies (50 and 200 Hz). The positions of the lines $A_1 - B_1$, $A_2 - B_2$ and $A_3 - B_3$ are depicted in Fig. 1.

The comparison shows good agreement between the computed results and the measurements. A more careful inspection of the results has revealed that the results of the $\boldsymbol{A} - \boldsymbol{T} - \boldsymbol{T}_0$ approach are slightly more accurate. The main purpose of this investigation was to assess the efficiency of both algorithms by comparing the computational times required to achieve a prescribed accuracy. Both calculations were performed on a worktop PC with a 2.93 GHz Intel Core Duo processor and 2 GB of RAM. In the case of the $\boldsymbol{A} - V$ approach the solution was reached after 6 h 23 min and 20 s for the case of frequency of 50 Hz, whereas computations using the $\boldsymbol{A} - \boldsymbol{T} - \boldsymbol{T}_0$ approach converged after only 19 min and 52 s. A significant reduction of the computing times of the FE equations using the $\boldsymbol{A} - \boldsymbol{T} - \boldsymbol{T}_0$ formulation compared with the $\boldsymbol{A} - V$ method has also been observed for the case when the system is supplied from a 200 Hz source; the

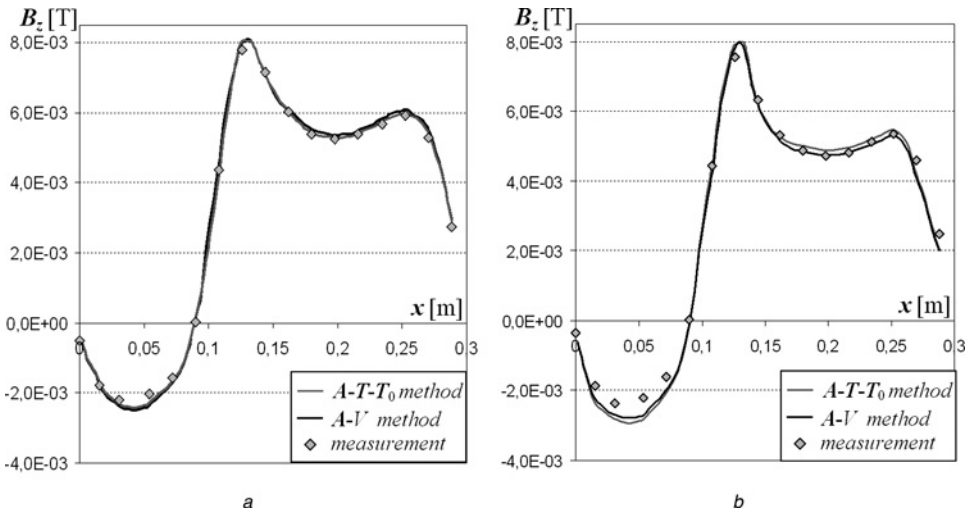

Fig. 6 *Magnitude of B_z along the line A_1–B_1 as shown in Fig. 1*

a 50 Hz
b 200 Hz

doi: 10.1049/iet-smt.2011.0114

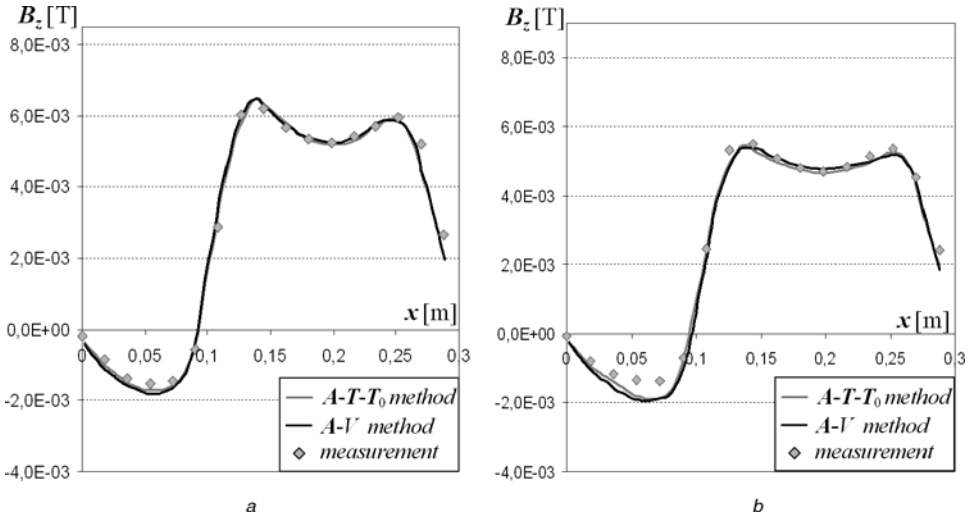

Fig. 7 *Magnitude of B_z along the line A_2–B_2 as shown in Fig. 1*

a 50 Hz
b 200 Hz

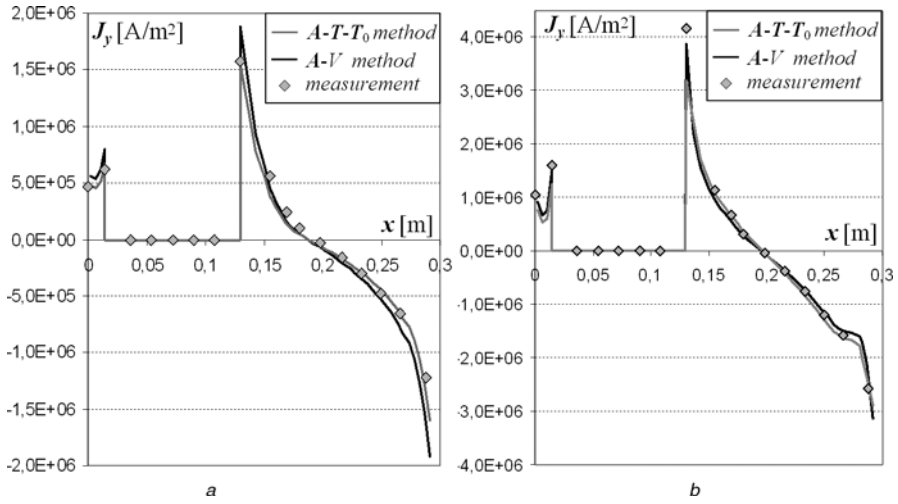

Fig. 8 *Magnitude of J_y along the line A_3–B_3 as shown in Fig. 1*

a 50 Hz
b 200 Hz

relevant times were 55 min 38 s using $\boldsymbol{A} - \boldsymbol{T} - \boldsymbol{T}_0$ and 2 h 44 min 14 s for $\boldsymbol{A} - V$, respectively.

6 Conclusions

The paper compares and contrasts two methods, the commonly employed $\boldsymbol{A} - V$ approach and a new formulation based on the vector potentials $\boldsymbol{A} - \boldsymbol{T} - \boldsymbol{T}_0$ adapted by the authors for problems with induced currents in multiply connected regions. Both methods yield similar accuracy of the solution, but the $\boldsymbol{A} - \boldsymbol{T} - \boldsymbol{T}_0$ approach is computationally much more efficient compared with the $\boldsymbol{A} - V$ formulation when applied to the problems containing conduction of multiply connected regions. It is acknowledged, however, that other solution methods exist for solving FE equations and thus a more comprehensive comparison and verification would be beneficial. The authors are currently developing a conventional ICCG implementation for solving the edge element equations of the $\boldsymbol{A} - \boldsymbol{T} - \boldsymbol{T}_0$ formulation to extend the base for comparisons.

7 References

1 Biro, O., Richter, K.: 'CAD in electromagnetism', *Adv. Electron. Electron Phys.*, 1991, **82**, pp. 1–96
2 Demenko, A., Sykulski, J.K., Wojciechowski, R.M.: 'Network representation of conducting regions in 3D finite element description of electrical machines', *IEEE Trans. Magn.*, 2008, **43**, (6), pp. 714–717
3 Bui, V., Le Floch, Y., Meunier, G., Coulomb, J.: 'A new three-dimensional (3D) scalar finite element method to compute T_0', *IEEE Trans. Magn.*, 2006, **42**, (4), pp. 1036–1038
4 Nakata, T., Takahashi, N., Fujiwara, K., Okada, Y.: 'Improvements of the T-Ω method for 3D eddy current analysis', *IEEE Trans. Magn.*, 1988, **24**, (1), pp. 94–97
5 Demenko, A., Sykulski, J.K., Wojciechowski, R.M.: 'Calculation of induced currents using edge elements and T–T_0 formulation', *IET Sci. Meas. Technol.*, 2008, **2**, (6), pp. 434–439
6 Turner, L., *et al.*: 'Workshops and problems benchmarking eddy current codes. TEAM Workshops: test problem 7' (Argonne, Illinois, 1988)

7 Demenko, A., Sykulski, J.K.: 'Network equivalents of nodal and edge elements in electromagnetics', *IEEE Trans. Magn.*, 2002, **38**, (2), pp. 1305–1308
8 Ren, Z., Qu, H.: 'Investigation of complementarity of dual eddy current formulations on dual meshes', *IEEE Trans. Magn.*, 2010, **46**, (8), pp. 3161–3164
9 Demenko, A.: 'Description of electrical machine windings in the finite element space', *COMPEL*, 2008, **27**, (4), pp. 711–719
10 Demenko, A., Wojciechowski, R.M.: 'Loop analysis of multi-branch, multi-node nonlinear circuits using singular formulation', *COMPEL*, 2009, **28**, (3), pp. 691–699
11 Biro, O., Preis, K., Richter, K.: 'On the use of magnetic vector potential in the nodal and edge element analysis of 3D magnetostatic problems', *IEEE Trans. Magn.*, 1996, **32**, (3), pp. 651–654
12 Demenko, A., Nowak, L., Pietrowski, W., Stachowiak, D.: '3D edge element method analysis of saturation effects in a permanent magnet machine', *COMPEL*, 2002, **21**, (1), pp. 126–137
13 Van der Vorst, H.A., Melissen, J.B.: 'A Petrow–Galerkin type method for solving $Ax = b$, where A is symmetric complex', *IEEE Trans. Magn.*, 1990, **26**, (2), pp. 706–708
14 Nakata, T., Fujiwara, K.: 'Results for benchmark problem 7', *COMPEL*, 1990, **9**, (3), pp. 137–154

doi: 10.1049/iet-smt.2011.0114